

Snowflake Divertor Plasmas on TCV

F. Piras, A. Bencze, S. Coda, B.P. Duval, I. Furno, J-M. Moret, R.A. Pitts¹, O. Sauter, B. Tal²,
D. Wagner, F. Felici, B. Labit, J. Marki, Y. Martin, S. Medvedev, A. Pitzschke, A. Pochelon,
G. Turri, C. Zucca and the TCV Team

Ecole Polytechnique Fédérale de Lausanne (EPFL)

Centre de Recherches en Physique des Plasmas (CRPP)

Association Euratom Confédération Suisse, Station 13, CH-1015 Lausanne, Switzerland

¹ *ITER Organization, Cadarache, F-13108, St Paul-lez-Durance, France*

² *KFKI-Research Institute for Particle and Nuclear Physics
EURATOM Association, PO Box 49, 1525 Budapest, Hungary*

Introduction

In future experimental nuclear fusion reactors, power exhaust handling and plasma wall interaction must be controlled to a level compatible with wall materials. This drives tokamak operation towards highly radiative edges. On the other hand, radiation in the core plasma should be minimized to improve the overall performance.

Different solutions have been proposed to reduce the plasma-wall interaction by acting on the magnetic field topology in diverted plasmas [1–4]. One of these solutions is the so-called snowflake (SF) divertor [1, 2]. The basic concept of the snowflake divertor (SF) is illustrated in Fig. 1.

In a standard X-point configuration (not shown here) the poloidal magnetic field vanishes at the null point (first order null). An SF diverted configuration is characterized by a second order null, i.e. the first derivatives of the magnetic field also vanish at the null point and the separatrix divides the poloidal plane into six sectors, Fig. 1(b). Perturbing the exact SF configuration produces the magnetic configurations which are respectively shown in Fig. 1(a) and Fig. 1(c). In these two configurations, the first derivatives of the poloidal magnetic field are small compared to those of a standard X-point (single null configuration, SN). Following Ref. [1, 2], we will refer to these two configurations as of snowflake-plus (SF+) and snowflake-minus (SF-) respectively.

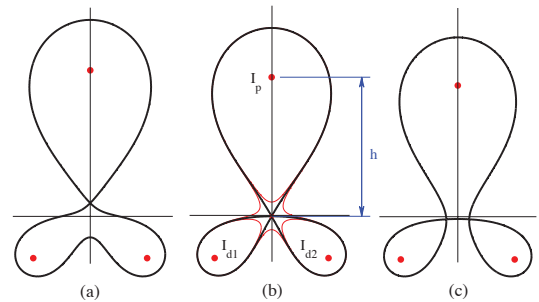


Figure 1: SF configurations in a straight tokamak model. The circles represent the current filaments (plasma, I_p , and divertor conductors, $I_{d1,2}$) and the bold black line is the separatrix.

The second order null modifies the magnetic topology near the plasma boundary and is therefore expected to affect the plasma properties in the scrape-off layer (SOL). The magnetic shear at the edge where the pedestal lies is also modified, providing a possible way to influence Edge Localized Modes (ELMs) activity in H-modes. Squeezing the flux tubes near the null point may also decouple the turbulence in the divertor legs and in the SOL and change the radial blob motion.

SF experiments on TCV

All three SF configurations have been created and controlled on the TCV tokamak [5], as shown in Fig. 2, demonstrating the feasibility of such plasmas.

Although the CCD images in fig. 2 are saturated, the visible emission qualitatively confirms the SF configurations reproduced by the magnetic reconstruction code.

The magnetic properties of the SF configurations are compared with those of the SN configuration using the magnetic measurements from the equilibria in Fig. 2.

For the SOL, an important parameter is the flux expansion. This quantity is related to the reduction of the poloidal magnetic field near the null point. The flux expansion influences the SOL thickness and the size of the radiating volume. Radial transport, and possibly formation of filaments in the edge/SOL region, may also be influenced by this flux expansion. For a given flux surface, the flux expansion is defined as the ratio $\psi_{exp} = \frac{\Delta}{R - R_{sep}}$, where Δ is the minimum distance between the X-point and the considered magnetic field line, and $R - R_{sep}$ is the distance between the same field line and the separatrix at the outer midplane.

In Fig. 3, the flux expansion for the SF configurations and for the SN configuration are plotted as a function of the distance $R - R_{sep}$. In the same figure, the connection length from the equatorial plane to the point closest to the x-point (CLx) is also shown. The connection length

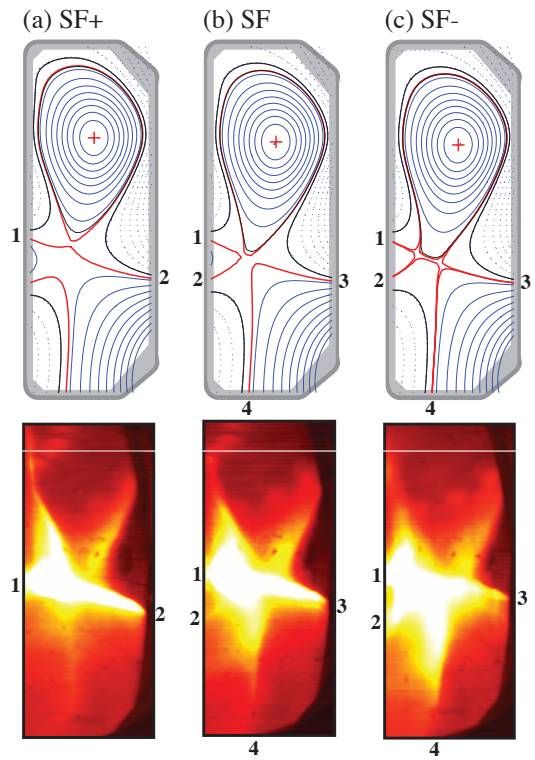


Figure 2: Equilibrium reconstructions and images from the tangential visible CCD camera for the SF configurations.

determines the residence time of a particle in the SOL and therefore affects the radiative losses and the thermal power to the divertor plates (the thickness of the SOL at the outer midplane is typically ~ 2 cm). The SF configuration has a flux expansion near the separatrix (Near SOL) and a connection length over twice larger than that of the SN. The SF+ and the SF- have similar values of flux expansion and connection length, with values that fall between the values computed for the SF configuration and the SN configuration.

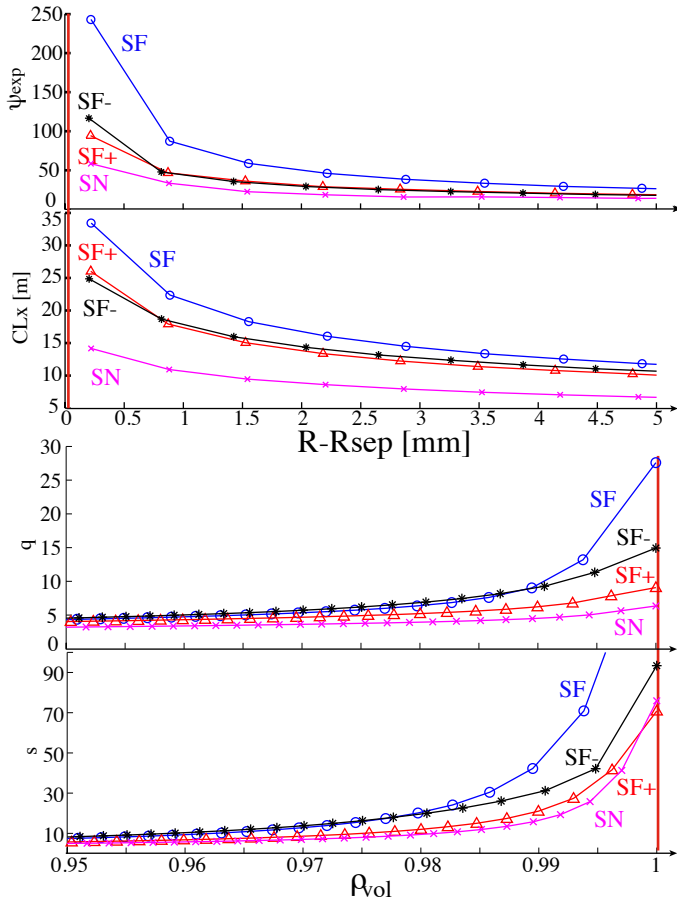


Figure 3: Flux expansion, connection length, q -profile and magnetic shear for the three SF configurations and an SN configuration.

files of the SF- are very similar to the SF up to $\rho_{vol} \simeq 0.985$ but then become closer to the SF+ and the SN. This might lead to differences in the MHD stability limits in between the SF+ and SF- which will be investigated in the future.

H-mode experiments in an SF configuration

The MHD stability limits of the SF configuration were computed and compared to those of a

The safety factor profile (q) and the magnetic shear ($s = \frac{\rho_{vol}}{q} \frac{dq}{d\rho_{vol}}$) are computed using the CHEASE code [6] and are also shown in Fig. 3. The LCFS used to compute these quantities ($\rho_{vol} = 1$) is just inside the separatrix to avoid the singularity of q and s at the null point. The SF configuration has a larger magnetic shear than that for the SN configuration. This difference is important for $\rho_{vol} > 0.96$. The SF+ and the SF- configurations have also a larger magnetic shear compared to the SN configuration. In the case of the SF- configuration, the presence of a double null in the separatrix results in a large volume where the poloidal magnetic field is small. This property emphasizes a dissimilarity in the magnetic shear profile compared with the SF+ configuration. Note that the pro-

SN configuration [7, 8]. It was found that the SF configuration does not degrade edge MHD stability and that the current driven kink modes of medium n are even more stable compared to the SN configuration.

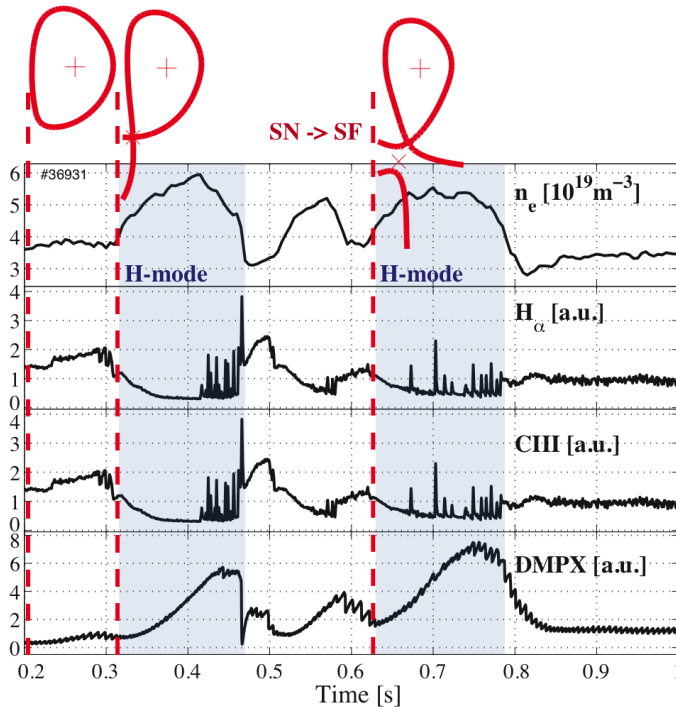


Figure 4: Electron plasma density (n_e), H_α and C-III radiation and soft-X radiation (DMPX signal) during an H-mode in both an SN and an SF configurations.

More experiments are planned to investigate the pedestal stability in an H-mode SF configuration.

This work was supported in part by the Swiss National Science Foundation

References

- [1] D. D. Ryutov et al, Phys. Plasmas **14** 064502 (2007)
- [2] D. D. Ryutov et al, Phys. Plasmas **15** 092501 (2008)
- [3] A. S. Kukushkin et al, Nucl. Fusion **55** 608-616 (2005)
- [4] M. A. Mahdavi et al, Phys. Rev. Lett. **47** 1602 (1981)
- [5] F. Piras et al, Plasma Phys. Control. Fusion **51** 055009 (2009)
- [6] H. Lütjens et al, Comput. Phys. Commun. **97** 219 (1996)
- [7] A. Pitzschke et al, SSP-09 Conference (2009)
- [8] S. Medvedev et al, EPS-09 Conference (2009)

Starting from these theoretical results, an experimental campaign on TCV as been undertaken to verify the accessibility of the H-mode with SF configurations.

In fig. 4, the electron plasma density n_e , the H_α and the C-III radiation and the soft-X radiation is plotted for an ohmic plasma discharge. During this experiment, the plasma configuration is modified; starting from a limited plasma, a SN configuration is created at $t = 0.31s$ and finally at $t = 0.62s$ the SF+ configuration is achieved. In spite of the small input power ($I_P = 300kA$, $P_{in} \sim 400kW$), an ELMy H-mode regime is observed in both the SN configuration and the SF configuration.